Published in final edited form as:
Cell. 2008 April 4; 133(1): 164–176.

Rapid synthesis of auxin via a new tryptophan-dependent pathway is required for shade avoidance in plants

Yi Tao[1,2], **Jean-Luc Ferrer**[3,4], **Karin Ljung**[5], **Florence Pojer**[1,4], **Fangxin Hong**[1,2,6], **Jeff A. Long**[2], **Lin Li**[2], **Javier E. Moreno**[7], **Marianne E. Bowman**[1,4], **Lauren J. Ivans**[2,8], **Youfa Cheng**[8], **Jason Lim**[1,2], **Yunde Zhao**[8], **Carlos L. Ballaré**[7], **Göran Sandberg**[9], **Joseph P. Noel**[1,4], and **Joanne Chory**[1,2*]

1*Howard Hughes Medical Institute*

2*Plant Biology Laboratory, The Salk Institute for Biological Studies, La Jolla, CA 92037, USA*

3*Institut de Biologie Structurale CEA-CNRS-UJF, Laboratoire de Cristallographie et Cristallogenèse des Protéines, 41 Rue Jules Horowitz, 38027 Grenoble Cedex 1, France*

4*The Jack H. Skirball Center for Chemical Biology and Proteomics, The Salk Institute for Biological Studies, La Jolla, CA 92037 USA*

5*Umeå Plant Science Centre, Department of Forest Genetics and Plant Physiology, Swedish University of Agricultural Sciences, SE-901 83 Umeå, Sweden*

6*Department of Biostatistics and Computational Biology, Dana-Farber Cancer Institute, Harvard School of Public Health, 44 Binney Street Boston, MA 02115, USA*

7*Instituto de Investigaciones Fisiológicas y Ecológicas Vinculadas a la Agricultura (IFEVA), Consejo Nacional de Investigaciones Científicas y Técnicas, and Universidad de Buenos Aires, Avenida San Martín 4453, C1417DSE Buenos Aires, Argentina*

8*Division of Biological Sciences, Section of Cell and Developmental Biology, University of California, San Diego, La Jolla, CA 92093-0348*

9*Umeå Plant Science Centre, Department of Plant Physiology, Umeå University, SE-901 87 Umeå, Sweden*

SUMMARY

Plants grown at high densities perceive a decrease in the red to far-red (R:FR) ratio of incoming light, resulting from absorption of red light by canopy leaves and reflection of far-red light from neighboring plants. These changes in light quality trigger a series of responses known collectively as the shade avoidance syndrome. During shade avoidance, stems elongate at the expense of leaf and storage organ expansion, branching is inhibited, and flowering is accelerated. We identified several loci in *Arabidopsis*, mutations in which lead to plants defective in multiple shade avoidance outputs. Here we describe SAV3, an aminotransferase, and show that SAV3 catalyzes the formation of indole-3-pyruvic acid (IPA) from L-tryptophan (L-Trp), the first step in a previously proposed, but uncharacterized, auxin biosynthetic pathway. This pathway is rapidly deployed to biosynthesize auxin at the high levels required to initiate the multiple changes in body plan associated with shade avoidance.

*Address correspondence to: Joanne Chory, (858) 552-1148, (858) 558-6379 (fax), chory@salk.edu.

INTRODUCTION

The mechanisms by which organisms alter their growth and development in response to changes in their ambient environment are largely unknown. Plants exhibit an enormous array of phenotypic plasticity because most plant organs do not arise until after the seed germinates, allowing organ size and shape to be optimized to the local environment. Because they are sessile and photosynthetic, plants are especially attuned to their light environment. Light influences every developmental transition from seed germination and seedling emergence to flowering. For shade-intolerant plants, such as *Arabidopsis thaliana*, a reduction in the R:FR ratio of incoming radiation, which is caused by absorption of red light and reflection of far-red radiation by canopy leaves, signals the proximity of neighboring plants and triggers the shade avoidance syndrome (SAS). A common phenotype of the SAS is re-allocation of energy resources from storage organs to stems and petioles so that the plant outgrows its competitors. Other responses induced by reduction in R:FR ratio include increased leaf angle, accelerated leaf senescence and reduced deposition of fixed carbon to storage organs (Ballare, 1999). In response to prolonged shade, reproductive development is accelerated, potentially leading to decreased biomass and seed yield (Franklin and Whitelam, 2005). As such, the SAS, a strategy of major adaptive significance to plants growing in natural ecosystems, can significantly impact yield in high-density plantings typical of modern agriculture (Ballare et al., 1997; Izaguirre et al., 2006).

Changes in light quality are perceived by the phytochromes, a family of R/FR photoreceptors. *Arabidopsis* has 5 phytochromes, PHYA-PHYE. PHYB is the major phytochrome in light-grown plants and plays a predominant role in the SAS (Ballare, 1999). *phyB* mutants display a constitutive shade-avoiding phenotype that is characterized by long hypocotyls and petioles, reduced chlorophyll content, early flowering (Reed et al., 1993), and a reduced response to low R:FR (Halliday et al., 1994).

The events following photoreceptor excitation by changes in light quality are poorly understood. Analysis of the *Arabidopsis* transcriptome following transfer of plants to simulated shade (low R:FR) revealed a large number of shade-induced, early response genes (Devlin et al., 2003; Salter et al., 2003; Sessa et al., 2005). mRNA levels of several transcription factor genes increase within a few minutes of exposure to low R:FR light, and falls very rapidly after transfer from low to high R:FR light. A negative regulatory gene is also rapidly induced by low R:FR (Sessa et al., 2005), suggesting that there is a gas-and-brake mechanism that ensures that plants do not have an exaggerated response to shade.

Genes encoding metabolic enzymes or signaling components of several phytohormones are also among the early response genes, implicating a role for plant hormones in the SAS (Devlin et al., 2003). Brassinosteroids (BRs), auxin, ethylene and gibberellins appear to be involved in the SAS as mutants that are defective in the metabolism or signaling of these hormones either have reduced elongation growth in response to shade or can suppress the constitutive shade-avoiding phenotype of *phyB* (Hisamatsu et al., 2005; Kanyuka et al., 2003; Kim et al., 1998; Kurepin et al., 2007; Luccioni et al., 2002; Morelli and Ruberti, 2002; Neff et al., 1999; Peng and Harberd, 1997; Pierik et al., 2004). The role of auxin in the SAS has been explored most extensively. Several studies have shown auxin transport is required (Kanyuka et al., 2003; Morelli and Ruberti, 2000; Steindler et al., 1999) In addition, low R:FR induces the expression of many known auxin-responsive genes and it also arrests the growth of leaf primordia through auxin-induced cytokinin metabolism (Carabelli et al., 2007) These results suggest that a functional auxin signaling pathway is required to have a shade avoidance response. Recently, Kurepin *et al*. showed that prolonged growth in the shade resulted in changes in the levels of indole-3-acetic acid (IAA, an endogenous auxin) and other hormones, suggesting that light quality also influences auxin homeostasis (Kurepin et al., 2007).

Despite the ecological and economic impact of the SAS, little is known about the underlying mechanisms linking photoperception to changes in physiology and development. Here we describe a genetic screen in *Arabidopsis* for mutants unable to elongate in simulated shade light. One of the genes identified, *SAV3*, encodes a protein with a C-terminal alliinase/aminotransferase domain. We present multiple lines of evidence that indicate a role for SAV3 in a previously proposed, but genetically and biochemically undefined, IAA biosynthetic pathway from L-Trp. We show that within one hour after transferring seedlings from white light to shade, the levels of free IAA increase in wild-type (WT) owing to an increase in the rate of IAA biosynthesis; in contrast, IAA levels are reduced in *sav3* mutants and there is no significant change in IAA levels in response to shade. Our results suggest that certain growth responses require a higher threshold of available IAA. In addition, as other IAA biosynthetic pathways (Zhao et al., 2001) cannot compensate for the loss of the SAV3-dependent pathway, there may exist multiple functional pools of IAA in *Arabidopsis*.

RESULTS

Identification of *Arabidopsis sav* mutants

To identify *Arabidopsis* genes that are involved in the SAS, we performed a forward genetic screen for seedlings that did not elongate after transfer from continuous white light (Wc) to simulated shade light. Details of the screen are outlined in Fig S1A and B. Seedlings that appeared similar to WT in Wc but had shorter hypocotyls than WT in shade were identified as shade avoidance (*sav*) mutants. To eliminate mutants with light-independent elongation defects, we germinated the mutants in the dark and grew them for 4 days, conditions under which wild-type hypocotyls become long. Of the 47 lines, 30 were significantly shorter than WT in the dark and we reasoned that they were likely to contain mutations in components of the cellular machinery required for elongation growth. To test this idea, we identified the defective gene in the *sav2* mutant as *TUB4* (At5g44340), which encodes a β-tubulin isoform (Snustad et al., 1992).

Seventeen lines exhibited no or very minor phenotypes in the dark, while being significantly shorter than WT in simulated shade. Through map-based cloning, we identified the *SAV1* gene as *DWF4*, which encodes a C-22 hydroxylase involved in brassinosteroid biosynthesis; *sav1* is predicted to be a weak allele of *DWF4*. *SAV3* was defined by 3 alleles and we thus focused our studies on the analysis of this locus.

sav3 seedlings are defective in multiple, but not all, shade avoidance responses

sav3 mutants exhibit shorter hypocotyls than WT when grown in simulated shade (Fig. 1A, B) and partially suppress the constitutive shade avoidance phenotype of a *phyB* null mutant (Fig.S2A). The SAS is a complex syndrome, involving rapid changes in gene expression, elongation of petioles, changes in leaf shape and angle, and accelerated flowering, in addition to elongation of the primary stem. Figure 1D shows that *sav3-2* (a null allele, see below) seedlings have shorter petioles and larger leaf area than WT Col-0 plants when grown in shade. Further, when subjected to supplementary FR, *sav3-1* plants were shorter and had reduced leaf hyponasty as compared to WT (Fig.1D, S2B). Our results demonstrate that the *sav3-1* mutant fails to induce SAS in a controlled environment typically used to detect PHYB-mediated SAS responses in light-grown plants. However, *sav3* mutants flowered at the same time as WT when grown in simulated shade (data not shown), suggesting that the light quality-controlled flowering time pathway operates independently of other shade-regulated pathways (Cerdan and Chory, 2003).

SAV3 encodes a protein with a predicted alliinase C-terminal /aminotransferase domain

We identified SAV3 by map-based cloning (Lukowitz et al., 2000). *SAV3* encodes a protein with an alliinase C-terminal /aminotransferase class I and II domain (At1g70560, Fig.2A). Alliinase is a pyridoxal phosphate (PLP) enzyme that catalyzes the production of the characteristic flavor molecule of onion, garlic and other related alliums (Kuettner et al., 2002a; 2002b). *sav3-1* contains a G to A point mutation at the splice junction of the fourth intron, resulting in elevated levels of a longer *SAV3* transcript and a predicted C-terminal truncation in the SAV3 protein (Fig.S1C), which may explain the slightly different response of this allele in some experiments (e.g., Fig.3A). *sav3-2* contains a G to A mutation in the second exon, converting Trp39 to a stop codon, and does not accumulate SAV3 protein (data not shown). *sav3-2* is presumed to be a null allele. *sav3-3* harbors a G to A mutation in the fourth exon, which converts Gly250 to Ser. Defects in the three alleles were rescued by a genomic copy of *SAV3* (Fig. 2C) or when the full-length cDNA was over-expressed under the control of the CaMV 35S promoter (data not shown), further confirming that their shade avoidance phenotypes resulted from mutations in the *SAV3* gene.

SAV3 is a plant-specific gene. In *Arabidopsis*, it is one of a 5-member gene family (Fig.2A). Three family members contain an N-terminal extension, which is predicted to be a signal peptide (http://www.cbs.dtu.dk/services/TargetP/), suggesting that, like the onion or garlic alliinases, these enzymes may function in the vacuole. SAV3 does not contain this N-terminal extension. Consistent with this prediction, we found that the SAV3 protein was localized to the cytoplasm in transgenic lines over-expressing a SAV3-YFP fusion protein (Fig.2B). SAV3 shares limited homology with garlic alliinase (36% identical), although most of the residues present in the active site of garlic alliinase are conserved in SAV3 (data not shown). A PLP cofactor is required for the enzymatic activity of alliinase. We found that recombinant SAV3 apoprotein expressed in *E. coli* binds to PLP *in vitro*. To test whether PLP is also required for the function of SAV3, we generated mutations in the predicted PLP binding residue (K217G/K217R) and introduced these constructs into *sav3-2*. As shown in Fig 2C, the mutant genes did not rescue *sav3*, suggesting that PLP is required for the function of SAV3 and that SAV3 is likely to function as an enzyme.

sav3 mutants have reduced auxin levels and a diminished auxin response

Given *sav3*'s pleiotropic phenotype, its predicted protein structure and knowing that several plant hormones are involved in the SAS, we reasoned that SAV3 might be involved in the biosynthesis or metabolism of auxin, which can be derived from L-Trp. We tested the responses of *sav3* mutants to an auxin analog, picloram (Sorin et al., 2005). Under Wc, the responses of *sav3* mutants to various concentrations of picloram were similar to that of WT. Under simulated shade, we found that high concentrations of picloram fully rescued the short hypocotyl phenotype of *sav3* (Fig.3A). Picloram did not rescue *sav1-1*. To examine the ability of *sav3* to respond to increases in endogenous auxin, we tested the hypocotyl elongation response of *sav3* mutants to high temperature treatment, conditions known to increase free auxin levels (Gray et al., 1998). As shown in Fig.S2C, *sav3* mutants were defective in high temperature induced hypocotyl elongation, whereas *sav1* had a response similar to WT. These results suggest that SAV3 is involved in auxin homeostasis.

To investigate whether endogenous auxin levels were altered in *sav3*, we measured free IAA levels in 7-day-old WT and *sav3* seedlings grown in Wc. *sav3* seedlings had about 60% of wild-type levels of auxin. To assess the influence of light on auxin levels, WT and *sav3* seedlings were grown in Wc and then transferred to shade for 1 hr. As shown in Fig3C, simulated shade treatment increased free IAA levels significantly in WT, but to a much lesser extent in *sav3-2*, suggesting that SAV3 is involved in shade-induced auxin production.

To assess the source of the shade-induced increase in free IAA, we performed a deuterium dioxide feeding experiment to measure the IAA biosynthesis rate. As shown in Fig.3D, the rate of IAA biosynthesis in Wc is similar in WT and *sav3* mutants. However, after 2 hours of shade treatment, an increase in IAA biosynthesis rate was detected in WT but not *sav3*, (indicated by the higher ratio of the deuterium labeled vs. unlabelled IAA). These results show that SAV3 is directly involved in shade-induced *de novo* IAA biosynthesis.

To better understand the molecular consequences of reduced auxin levels, we interrogated the transcriptome of WT and *sav3-2* seedlings before and after 1 hr of simulated shade using the Affymetrix® ATH1 array (data submitted to GEO, GSE9816). RNA was prepared from whole seedlings of WT, *sav3-2* and *sav1-1* grown in simulated Wc for 7 days and either left in Wc or transferred to simulated shade (R:FR = 0.7) for 1 hr. *sav1* was included as a control for specificity. Comparisons of genotypes and treatments were performed using the RankProd package from Bioconductor (Hong et al., 2006). At a 5% false discovery rate, the levels of 80 transcripts were increased in the WT following shade treatment. The expression patterns of these genes are shown in Fig.4A. The majority of genes that were up-regulated by shade in WT plants had reduced expression in shade-treated *sav3* mutants, although there were some notable exceptions, e.g., the known shade-up-regulated genes, PAR1, HFR1, and ATHB2 (Fig.S3A). The expression of the shade up-regulated genes in *sav1* was similar to WT. We carried out a similar analysis to identify genes that were differentially expressed in shadetreated WT and *sav3*. 66 genes were found to be expressed at significantly lower levels in *sav3* compared to WT, of which 36 were among the list of 80 genes identified as shade up-regulated in WT. We performed co-response analysis of these 36 genes using data from Genevestigator V2 (https://www.genevestigator.ethz.ch/at/, Fig.4B). We found that most of these genes were also up-regulated by IAA, but not other hormones, indicating that the *sav3* mutation specifically affects the induction of auxin-responsive genes.

To validate the microarray results, we selected two genes (*IAA19* and *IAA29*), whose expression was up-regulated by shade in WT, but not in *sav3-2*. Using quantitative PCR, we showed that the shade-induced induction of these two genes was reduced in *sav3-1, sav3-2, and sav3-3* (Fig.4C). Moreover, this reduction could be rescued by treating *sav3* mutants with 1 μM of IAA (Fig.S3B). These data support the hypothesis that *SAV3* is involved directly in auxin biosynthesis. Additionally, since *SAV3* is required for shade-induced gene expression as early as 1 hr after transfer to shade, we conclude that changes in auxin levels are required for the primary responses of the SAS.

SAV3 has a localized and dynamic expression pattern

To further explore the connection between auxin and SAV3, we examined the expression pattern of *SAV3*. Transgenic lines expressing a SAV3-GUS fusion protein under the control of a 2Kb *SAV3* promoter were generated. In 5-day-old seedlings, expression of *SAV3* in the shoot was observed mainly in the emerging young leaves, at the leaf margin and in the vasculature. In roots, it was expressed in the quiescent center and in the vasculature of root tips (Fig.5A; data not shown).

During embryogenesis, the expression pattern of *SAV3* changes dynamically. Using *in situ* hybridization, *SAV3* mRNA accumulation was first detected at the 32 to 64-cell stage of embryogenesis. Initially, *SAV3* was expressed strongly in the most apical 3 to 4 cells of the epidermis and was weakly expressed in the cells that give rise to the vasculature of the hypocotyl. By the heart stage of embryogenesis, *SAV3* was strongly expressed in the developing vasculature and was detected in the derivatives of the hypophyseal cell that gives rise to the quiescent center of the root. *SAV3* was also expressed in the apical epidermal layer (Fig.5B). At the torpedo stage of embryogenesis, *SAV3* expression was detected in the developing vasculature of the root, hypocotyl and cotyledons, as well as in the L1 layer of the presumptive

shoot apical meristem and the adaxial epidermis of the developing cotyledons (Fig.5D). In 5-day-old seedlings, *SAV3* expression was maintained in the L1 of the shoot apical meristem and was detected in the developing vasculature of leaf primordia (data not shown).

Of interest, the expression pattern of *SAV3* in the shoot was similar to that of DR5::GUS, an artificial auxin reporter gene construct, whose expression is thought to reflect the levels of free auxin (Aloni et al., 2003; Cheng et al., 2006; Mallory et al., 2005; Sabatini et al., 1999). Although *sav3* is defective in shade-induced hypocotyl elongation, we observed little expression of *SAV3* in hypocotyls of 5-day-old seedlings. We found that shade treatment did not alter the expression pattern of *SAV3* (Fig.5A), rather it reduced the expression of *SAV3* after 2 hrs of shade treatment (Fig.S4A), suggesting a possible feedback regulation on *SAV3* expression by shade. DR5::GUS expression levels increased in cotyledons after 8 hours of shade treatment, but we detected no GUS activity in hypocotyls at this time point. To investigate the site of auxin accumulation in Wc and following shade treatment, we dissected hypocotyls from other aerial tissues in WT harboring a DR5::GUS reporter. We found that after 4 hrs of shade treatment, GUS activity increased in both hypocotyls and the other aerial tissues (Fig. 5D). However, in the presence of 5 μM NPA, an auxin transport inhibitor, the increases of GUS activity caused by shade were not observed in hypocotyls, while increased GUS activity was still observed in the other aerial tissues. This indicates that the main source of new auxin is in leaves, where *SAV3* is highly expressed; auxin is then transported to sites of elongation growth, such as hypocotyls.

SAV3 is an L-Trp aminotransferase involved in IAA biosynthesis

Because SAV3 is annotated as containing an aminotransferase domain and *sav3* mutants have reduced auxin, we investigated whether L-Trp, an IAA biosynthetic precursor, serves as an *in vitro* substrate of SAV3. Several Trp-dependent auxin biosynthetic pathways have been proposed in *Arabidopsis*: the indole-3-acetamide (IAM) pathway, the tryptamine pathway, the indole-3-acetaldoxime (IAOx) pathway and the indole-3-pyruvic acid (IPA) pathway (Fig.6A). While there is evidence for the IAOx and tryptamine pathways, the IPA pathway remains conjecture. Since PLP-utilizing enzymes can catalyze a variety of reactions including transaminations, racemization, decarboxylation, and side-chain eliminations or replacements (Aitken and Kirsch, 2005;Dunathan, 1966), we tested whether SAV3 could catalyze the formation of IPA from L-Trp. Using bacterial- expressed recombinant SAV3 protein, we found that, when supplied with sodium pyruvate or α-ketoglutarate as co-substrates for PLP-dependent transamination reactions, SAV3 produced IPA from L-Trp but not from D-Trp. The production of IPA was confirmed using LC/MS (Fig.6B). This result suggests that SAV3 is involved in IPA-dependent auxin biosynthesis.

We further characterized the biochemical properties of SAV3 and found that the optimal temperature for SAV3 catalyzed IPA production was 55 °C; the optimal pH was 8.8 (Fig.S5A). SAV3 has an apparent Km for L-Trp of 0.29 mM and a Vmax of 12.9 μM/min (Fig.7A). To test the substrate specificity of SAV3, we examined the aminotransferase activity of SAV3 towards other amino acids. In our assays, SAV3 also used L-Phe, Tyr, Leu, Ala, Met and Gln as substrates (Fig.S5B). To investigate whether SAV3 uses L-Trp as a substrate *in vivo*, we examined the susceptibility of *sav3* to the toxic Trp analog: 5-methyl tryptophan (5-MT) (Zhao et al., 2001). Enzymes that use Trp as a substrate can metabolize 5-MT; thus, mutations in these enzymes give rise to plants that are hypersensitive to 5-MT. Indeed, when grown on 20 μM 5-MT in Wc, *sav3-2* was more susceptible to 5-MT than WT seedlings, suggesting that SAV3 is involved in Trp-dependent auxin biosynthesis *in vivo* (Fig.7B). A role for *SAV3* in auxin biosynthesis was further supported by expressing the bacterial auxin biosynthesis gene, *iaaM*, under the control of the *SAV3* promoter, which should increase auxin levels at sites where

SAV3 is expressed (Cheng et al., 2006). We found that expression of *iaaM* caused a long hypocotyl phenotype in both WT and *sav3-2*, regardless of the light condition (Fig.S4B).

To further examine whether L-Trp is the preferred substrate of SAV3, we performed an *in silico* docking experiment using the crystal structure obtained from SAV3 crystals soaked in L-Phe and co-crystallized with PLP (PDB code: 3bwn) (J.-L. Ferrer et. al., in preparation). We found that the structure of SAV3 shares a degree of homology with alliinase from *Allium sativum* (garlic), for which the structure of both the apo form and the ternary complex with the aminoacrylate reaction intermediate covalently bound to the PLP cofactor are available (PDB code: 1lk9, 2hor and 2hox). We computationally tested L-Trp, Phe, Tyr and His covalently tethered to PLP through their respective amino groups as Schiff bases on a model of SAV3 free of the PLP co-factor normally found associated with SAV3 crystal structures (J.-L. Ferrer et al., in preparation). After computational energy minimization and *in silico* structure refinement using the program Glide (part of the Schrödinger^{TM} suite, www.schrodinger.com), all refined docking complexes resulted in the PLP co-factor bound at the same position as observed in the experimental crystal structures (Fig.7C). Notably, the L-Trp-PLP adduct scored highest in this computational run. In addition, the carboxyl groups of both L-Trp-PLP and the aminoacrylate-PLP complexes point towards a conserved Arg residue that resides in the same three-dimensional locations of the superimposed structures of SAV3 and alliinase (Fig.7C: Arg363 in SAV3 and Arg401 in alliinase). The consistency between the computational results and experimental structures validates our docking results. We also examined computationally IPA, L-Trp, Tyr, Phe, His as well as D-Trp on a model of SAV3 now containing PLP. IPA docking resulted in the best score followed by L-Trp and then L-Phe, L-Tyr, L-His, and D-Trp scored the lowest. Independent of prior knowledge, we also completed a large *in silico* docking experiment with a small molecule library (http://blaster.docking.org/zinc/choose.shtml). Notably, the best scoring small molecules possessed chemical structures similar to the presumptive SAV3 reaction product IPA (Ferrer et al., in preparation). In summary, the *in silico* computational docking experiments support the hypothesis that L-Trp serves as the preferred physiological substrate of SAV3 while IPA is the expected product.

DISCUSSION

Identification and biochemical characterization of SAV3 supports the existence of a new Trp-dependent IAA biosynthetic pathway in higher plants

Despite the central role of auxin in plant growth and development, details of how auxin is synthesized continue to puzzle plant biologists. Multiple Trp-dependent pathways and a Trp-independent pathway for the production of IAA have been proposed to function in higher plants (Woodward and Bartel, 2005). Through forward genetics, several auxin overproduction mutants have been identified; however, very few auxin-deficient mutants—which are critical for evaluating the function of each proposed pathway—have been reported. None of the pathways have been characterized completely, either in terms of detecting the proposed biosynthetic intermediates or identifying the enzymes that catalyze each step. In addition, the specific role of each pathway *in planta* and how these biosynthetic pathways intersect and are regulated are not known.

Of the multiple pathways proposed for the biosynthesis of IAA, the IPA pathway (L-Trp to IPA, to indole-3-acetaldehyde (IAAld), to IAA) is the least characterized. Mutations in *yucca* genes identified a set of related enzymes that convert tryptamine to N-hydroxyl tryptamine in the IAOx pathway (Fig.6A, (Zhao et al., 2001)) Despite their clear role in auxin biosynthesis, mutations in these enzymes do not result in decreased endogenous pools of IAA in mutant plants. Likewise, mutations in nitrilases do not lead to decreased accumulation of IAA (Fig.6A). So far, only one auxin-deficient mutant in *Arabidopsis* has been described to

have significantly reduced free IAA levels due to mutations in enzymes involved in Trp-dependent IAA biosynthesis pathway (Zhao et al., 2002). This double mutant, lacking two cytochrome P450 genes, *cyp79b2/cyp79b3*, shows a significant reduction in free IAA levels when grown at 26°C, although levels are not significantly different from WT when plants are grown at lower temperatures, conditions in which *Arabidopsis* normally is found.

We provide multiple lines of evidence that SAV3 is an aminotransferase specifically involved in the formation of IPA from L-Trp in an IAA biosynthetic pathway. *sav3* mutants fail to up-regulate scores of auxin-inducible genes during shade avoidance, accumulate approximately half the amount of free IAA compared to WT, do not increase IAA biosynthesis rates as WT plants do in response to shade, and are hypersensitive to a toxic Trp analog. Second, SAV3 catalyzes the formation of IPA from L-Trp *in vitro*. In other studies, we determined the 3-D structure of SAV3 (J.L. Ferrer et al. in preparation). We used this information to model the active site of SAV3, and show here that L-Trp and IPA dock into the SAV3 active site with the lowest energies and in conformations consistent with the expected enzymatic mechanism for PLP-dependent transamination. Together with quantitative *in vitro* biochemical assays, these series of computational experiments constitute reliable evidence that L-Trp is the *in vivo* substrate of SAV3, even though SAV3 and other aminotransferases are known to turnover a number of related uncharged and hydrophobic amino acids with reduced catalytic efficiency (Soto-Urzua et al., 1996).

An IPA-dependent IAA biosynthetic pathway has been characterized in several bacteria (Badenoch-Jones, 1982; Kaneshiro, 1983). IPA has been identified from several plant species; however, the existence of an IPA-mediated IAA biosynthetic pathway has not been shown, which may be due to the instability of IPA (Tam and Normanly, 1998). The identification of SAV3 as the Trp aminotransferase of the IPA-pathway indicates that this pathway is operative in *Arabidopsis*. SAV3 has a relatively high apparent Km for L-Trp (0.29 mM), comparable to the activities reported in crude extracts of *Phaseolus aureus* (0.33mM), in tomato shoots (5 mM), or in bacteria (1.05 to 3.3mM). In *Enterobacter cloacae*, a Trp aminotransferase has a Km of 3.3 mM for L-Trp and 24 μM for IPA and it was hypothesized that the low affinity of the enzyme for L-Trp and the high affinity for the product may reflect the need to maintain low intracellular IPA levels (Koga et al., 1994). Most enzymes operating under near steady state physiological conditions maintain Km values that approximate the available concentration of substrate. In the case of SAV3, the localized concentration of L-Trp may serve as an exquisitely fine-tuned control point for time and spatially dependent auxin production. Knowledge of the temporal and spatial concentrations of substrates and intermediates of the IPA-dependent IAA biosynthetic pathway together with quantitative descriptions of IAA biosynthetic enzymes should shed light on the regulatory functions of enzymes such as SAV3 in plant development.

SAV3 shares properties reported for Trp aminotransferases measured in crude extracts from multiple organisms. SAV3 can utilize all of the aromatic amino acids as well as Leu, Ala and Met as substrates, as can those from *Phaseolus* and *Azospirillum brasilense* (Baca, 1994; Truelsen, 1972). However, SAV3's Km for L-Tyr and L-Phe is 4.96 mM and 9.08 mM (Fig.S5C), respectively, while under the same conditions, the Km for L-Trp is 0.29 mM. Thus, L-Trp is likely to be the preferred substrate for SAV3.

In bacteria, IPA decarboxylase (IPDC) is believed to be the key enzyme for the IPA-dependent IAA biosynthetic pathway because the other two enzymes, Trp aminotransferase and indole-3-acetaldehyde oxidase, are present in most bacteria including those that are incapable of producing IAA (Koga et al., 1991; 1992; 1994). In *Enterobacter cloacae*, IPDC catalysis is the rate-limiting step in the production of IAA (Koga et al., 1994). This biosynthetic bottleneck may also be shared in the higher plant pathway as we found that over-expression of SAV3 did

not result in an auxin overproduction phenotype; *SAV3* over-expression also did not enhance hypocotyl elongation in shade, suggesting that SAV3 is unlikely to be a rate-limiting enzyme in the higher plant IPA-dependent IAA biosynthetic pathway. As such, identification of a plant IPDC is a top priority.

Auxin biosynthetic pathways are not redundant

The difficulty in genetically dissecting auxin biosynthetic pathways has been attributed to the redundancy of auxin biosynthetic genes and the existence of multiple routes to IAA (Cheng et al., 2006; Woodward and Bartel, 2005). When grown at 22°C in Wc, 7-day old seedlings carrying a null allele of *sav3* appear generally similar to WT, even though *sav3* mutants contain only 60% of wild-type levels of free auxin. This suggests that under such growth conditions, auxin is not limiting. However, when seedlings are transferred to shade, the rate of IAA biosynthesis increases dramatically in WT, but not in *sav3* seedlings. As such, when *Arabidopsis* encounters shade similar to our conditions, other Trp-dependent IAA biosynthesis pathways, such as the *YUCCA*-dependent pathway, cannot compensate for loss of the IPA pathway. We noticed that *YUC 2,5,8* and *9* were induced by low R:FR in our array data (Fig.S6A). We thus examined the shade phenotypes of the corresponding *yuc* mutants and a *yuc* 3,5,7,8,9 quintuple mutant. We did not see any defect in shade induced hypocotyl elongation (Fig.S6B), indicating that these *YUC* genes are not required for the SAS in our conditions.

We offer several alternatives to explain this observation. In the first, IAA biosyntheti enzymes may accumulate in spatially or temporally distinct patterns during development. In support of this, members of the *YUCCA* gene family (Cheng et al., 2006) and *SAV3* are expressed in discrete and dynamic patterns during development. Further analysis is required to spatially refine the degree of overlap in expression at the cell type level. It is also possible that there are separate pools of IAA in plants and one pool is not available to compensate for the loss of another (Jones et al., 1991). In addition, the subcellular localization of IAA biosynthetic enzymes might lead to localized production, and perhaps a distinct pool, of auxin within a cell. It is important to point out that the complete set of enzymes for a particular pathway from Trp to IAA has not been isolated. Thus, in each cell type, which Trp-dependent pathway(s) is utilized to synthesize IAA remains unknown.

The SAV3 pathway can be rapidly deployed to increase auxin levels in response to shade

Here we show that mutations in *SAV3* alone lead to a dramatic reduction in free IAA levels, suggesting that IPA-dependent IAA biosynthesis is an important pathway for the biosynthesis of free IAA. In addition, SAV3 is required for the rapid increase in auxin levels through *de novo* IAA biosynthesis upon exposure to shade. This increase in free IAA is a prerequisite for the induction of a large number of auxin-regulated genes and is required for the full implementation of the SAS. Notably, cells with the highest expression levels of *SAV3* are distinct from the ones that show maximal elongation growth in response to low R:FR. This is consistent with previous reports in which auxin transport is required for low R:FR induced hypocotyl elongation (Steindler et al., 1999), and for the induced expression of some shade-induced marker genes in stem, the photoreceptive sites in shoots are in cotyledons, not in hypocotyls (Tanaka et al., 2002). Thus, we propose that the low R:FR signal is perceived by phytochrome in cotyledons or leaves where *SAV3* is highly expressed. SAV3 then mediates a transient increase in free IAA, which is transported to hypocotyls, leading to the up-regulation of auxin-responsive genes involved in elongation growth. In support of this model, we found that an auxin transporter inhibitor, NPA, can block the shade-induced increase of a DR5::GUS reporter in hypocotyls, indicating that shade induced increases in auxin biosynthesis occur in the upper part of the shoot, and auxin is transported to the hypocotyls where it participates in a growth response.

Conclusions

Our data show that SAV3 is a key enzyme required for rapid shade-induced changes in auxin levels. SAV3 is critical for the initiation of and full induction of shade avoidance responses in *Arabidopsis*. Identification of this enzyme, both in our screen and in the screen described in the accompanying paper by Stepanova et al. (2008) provides evidence that the proposed IPA-dependent IAA biosynthetic pathway operates in higher plants. Because the two screens identified the same Trp-aminotransferase, we propose that the gene be renamed *TAT1* (*TRYPTOPHAN AMINOTRANSFERASE1*) in future publications. The TAT1-dependent pathway is a major production route of free IAA in *Arabidopsis*, and appears to be required to rapidly increase free IAA levels in response to environmental changes. Since IAA can be synthesized from Trp via other known pathways, our results suggest that certain growth responses,such as the SAS, require higher levels of free IAA than other auxin-dependent responses.

Experimental Procedures

Plant materials and growth conditions

EMS mutagenized M2 seeds of the WT accession, Col-0, were purchased from Lehle seeds (http://www.arabidopsis.com). The screen is outlined in Sup.1A. Seedlings were grown at 22 °C. Four light conditions were used: Wc: fluorescent light, 30–50 $\mu E \cdot m^{-2} \cdot s^{-1}$; simulated Wc: LED light, R: 13 $\mu E \cdot m^{-2} \cdot s^{-1}$ and Blue (B): 1.23 $\mu E \cdot m^{-2} \cdot s^{-1}$; simulated shade: simulated Wc light plus LED FR light: 20.2 $\mu E \cdot m^{-2} \cdot s^{-1}$ (R:FR ratio: 0.7); supplementary FR light: greenhouse light supplemented with FR filter covered incandescent light (R:FR ratio: 0.24 for +FR and 0.68 for −FR). (Details of this and other experiments are described in supplementary materials). Quantitative measurements of hypocotyls, petioles, and leaf area were performed on scanned images of seedlings using scion image software (http://www.scioncorp.com/). For all measurements, at least 12 seedlings were used per treatment or genotype. In all figures, error bar represents standard error. Construction of plasmids for complementation, SAV3 protein localization, and expression studies are described in detail in the Supplement. At least three lines were used for characterization. GUS staining was performed using 5-Bromo-4-chloro-3-indoxyl-beta-D-glucuronide cyclohexylammonium salt (Gold Biotechnology) as described (Jefferson et al., 1987).

Map-based cloning

Mutants were crossed to L*er* and the segregating F2 seedlings were screened for short hypocotyls in shade. The Monsanto *Arabidopsis* Polymorphism and L*er* Sequence Collections (http://www.arabidopsis.org/browse/Cereon/index.jsp) were used for designing SSLP, CAPS and dCAPS markers.

Gene Expression Profiling

Total RNA was extracted using Trizol (Invitrogen) and Biotin labeled using One-cycle target labeling kit (Affymetrix). Affymetrix ATH1 array was used according to the manufacturer's guidelines. Scanned arrays were analyzed with Affymetrix MAS 5.0 software and then normalized with gcRMA obtained from bioconductor (http://bioconductor.org/).

SAV3 activity assays

The 100 µl assay mixture contained 50mM L-Trp, 50mM sodium pyruvate, 100 µM PLP and 30 µg of purified SAV3 in reaction buffer (50mM K_2HPO_4/KH_2PO_4, pH 8.5). The reaction was incubated at 25 °C for 3 hours and then stopped by acidifying with 3M phosphoric acid to pH 3, followed by extraction with equal volume of ethyl acetate (3X). The supernatant was

dried and the pellet was resuspended in 30 µl of methanol. The ethyl acetate layer was collected, dried and re-suspended in 30 µl of methanol. The methanol solubilized extracts were analyzed by liquid chromatography (LC) on an Agilent 1100 HPLC using a chiralcel OD-RH column (0.46 cm I.D. × 15 cm) (Daicel Chemical Ind., LTD) at a flow rate of 0.5 ml/min, coupled to an electrospray ionization (ESI) XCT ion trap mass spectrometer XCT ion trap (Agilent) run in the negative-ion mode. Eluants were mixed with 20 mM ammonium acetate in 65% acetonitrile (100 µl/min) prior to injection in the mass spectrometer. A linear gradient of acetonitrile/0.1% formic acid (1–70%) in water/0.1% formic acid was used for column elution. The negative ion-ESI mass spectrum of IPA standards behaved as expected with a m/z = 202.2 ([M - H]-).

Biochemical characterization of SAV3 was performed using a borate buffer assay (Matheron and Moore, 1973). For 100 µl of reaction, 0.5 µg of SAV3 was used. The reaction was performed at 55 °C for 5 minutes (2min for kinetics). Km and Vmax were determined by Graphpad Prism® 5 software using non-linear regression for Michaelis-Menten equation.

Quantification of IAA

7-day old, Wc-grown Col-0 and *sav3-2* seedlings were used. For quantification of free IAA, they were treated with or without simulated shade for 1 hour and the aerial part of seedlings were weighed and collected. For IAA biosynthesis rate measurements, seedlings were pre-treated with ½ MS containing 30% ^2H_2O for half-an-hour and then subjected to Wc or shade for 2 hours. Aerial part of seedlings was collected. The measurements were performed as described (Ljung et al., 2005). For calculation of the relative synthesis rate of IAA, enrichment is expressed as the ratio of deuterium labeled IAA (*m/z* 203+204+205) to unlabeled IAA (*m/z* 202), after correction for natural isotope distribution to *m/z* 203, 204 and 205.

Supplementary Material

Refer to Web version on PubMed Central for supplementary material.

Acknowledgments

We thank Drs. Mark Estelle and Jose Alonso for sharing unpublished data. These studies were supported by NIH grant GM52413 (to J.C.), the Swedish research councils VR and Formas (K.L., G.S.) and the Howard Hughes Medical Institute (Y.T., J.L., J.P.N., J.C.).

References

Aitken SM, Kirsch JF. The enzymology of cystathionine biosynthesis: strategies for the control of substrate and reaction specificity. Arch Biochem Biophys 2005;433:166–175. [PubMed: 15581575]

Aloni R, Schwalm K, Langhans M, Ullrich CI. Gradual shifts in sites of free-auxin production during leaf-primordium development and their role in vascular differentiation and leaf morphogenesis in *Arabidopsis*. Planta 2003;216:841–853. [PubMed: 12624772]

Baca BE, Soto-Urzua L, Xochihua-Corona YG, Cuervo-Garcia A. Characterization of two aromatic amino acid aminotransferases and production of indole-3-acetic acid in *Azospirillum* spp. strains. Soil Biol Biochem 1994;26:57–63.

Badenoch-Jones J, Summons RE, Rolfe BG, Parker CW, Letham DS. Mass spectrometric identification of indole compounds produced by *Rhizobium* strains. Biomed Mass Spectrom 1982;9:429–437.

Ballare CL. Keeping up with the neighbours: phytochrome sensing and other signalling mechanisms. Trends Plant Sci 1999;4:97–102. [PubMed: 10322540]

Ballare CL, Scopel AL, Sanchez RA. Foraging for light: photosensory ecology and agricultural implications. Plant, Cell Environ 1997;20:820–825.

Carabelli M, Possenti M, Sessa G, Ciolfi A, Sassi M, Morelli G, Ruberti I. Canopy shade causes a rapid and transient arrest in leaf development through auxin-induced cytokinin oxidase activity. Genes Dev 2007;21:1863–1868. [PubMed: 17671088]

Cerdan PD, Chory J. Regulation of flowering time by light quality. Nature 2003;423:881–885. [PubMed: 12815435]

Cheng Y, Dai X, Zhao Y. Auxin biosynthesis by the YUCCA flavin monooxygenases controls the formation of floral organs and vascular tissues in *Arabidopsis*. Genes Dev 2006;20:1790–1799. [PubMed: 16818609]

Devlin PF, Yanovsky MJ, Kay SA. A genomic analysis of the shade avoidance response in *Arabidopsis*. Plant Physiol 2003;133:1617–1629. [PubMed: 14645734]

Dunathan HC. Conformation and reaction specificity in pyridoxal phosphate enzymes. Proc Natl Acad Sci USA 1966;55:712–716. [PubMed: 5219675]

Franklin KA, Whitelam GC. Phytochromes and shade-avoidance responses in Plants. Ann Bot (Lond). 2005

Gray WM, Ostpn A, Sandberg G, Romano CP, Estelle M. High temperature promotes auxin-mediated hypocotyl elongation in *Arabidopsis*. Proc Natl Acad Sci USA 1998;95:7197–7202. [PubMed: 9618562]

Halliday KJ, Koornneef M, Whitelam GC. Phytochrome B and at least one other phytochrome mediate the accelerated flowering response of *Arabidopsis thaliana L.* to low redfar-red ratio. Plant Physiol 1994;104:1311–1315. [PubMed: 12232170]

Hisamatsu T, King RW, Helliwell CA, Koshioka M. The involvement of gibberellin 20-oxidase genes in phytochrome-regulated petiole elongation of *Arabidopsis*. Plant Physiol 2005;138:1106–1116. [PubMed: 15923331]

Hong F, Breitling R, McEntee CW, Wittner BS, Nemhauser JL, Chory J. RankProd: a bioconductor package for detecting differentially expressed genes in meta-analysis. Bioinformatics 2006;22:2825–2827. [PubMed: 16982708]

Izaguirre MM, Mazza CA, Biondini M, Baldwin IT, Ballare CL. Remote sensing of future competitors: impacts on plant defenses. Proc Natl Acad Sci USA 2006;103:7170–7174. [PubMed: 16632610]

Jefferson RA, Kavanagh TA, Bevan MW. GUS fusions: beta-glucuronidase as a sensitive and versatile gene fusion marker in higher plants. EMBO J 1987;6:3901–3907. [PubMed: 3327686]

Jones AM, Cochran DS, Lamerson PM, Evans ML, Cohen JD. Red light-regulated growth. I. Changes in the abundance of indoleacetic acid and a 22-kilodalton auxin-binding protein in the maize mesocotyl. Plant Physiol 1991;97:352–358. [PubMed: 11538374]

Kaneshiro T, Slodki ME, Plattner RD. Tryptophan catabolism to indolepyruvic and indoleacetic acid by *Rhizobium japonicum* L-259 mutants. Curr Microbiol 1983;8:301–306.

Kanyuka K, Praekelt U, Franklin KA, Billingham OE, Hooley R, Whitelam GC, Halliday KJ. Mutations in the huge *Arabidopsis* gene *BIG* affect a range of hormone and light responses. Plant J 2003;35:57–70. [PubMed: 12834402]

Kim BC, Soh MS, Hong SH, Furuya M, Nam HG. Photomorphogenic development of the *Arabidopsis shy2-1D* mutation and its interaction with phytochromes in darkness. Plant J 1998;15:61–68. [PubMed: 9744095]

Koga J, Adachi T, Hidaka H. Molecular cloning of the gene for indolepyruvate decarboxylase from *Enterobacter cloacae*. Mol Gen Genet 1991;226:10–16. [PubMed: 2034209]

Koga J, Adachi T, Hidaka H. Purification and characterization of indolepyruvate decarboxylase. A novel enzyme for indole-3-acetic acid biosynthesis in *Enterobacter cloacae*. J Biol Chem 1992;267:15823–15828. [PubMed: 1639814]

Koga J, Syono K, Ichikawa T, Adachi T. Involvement of L-tryptophan aminotransferase in indole-3-acetic acid biosynthesis in *Enterobacter cloacae*. Biochim Biophys Acta 1994;1209:241–247. [PubMed: 7811697]

Kuettner EB, Hilgenfeld R, Weiss MS. The active principle of garlic at atomic resolution. J Biol Chem 2002;277:46402–46407. [PubMed: 12235163]

Kuettner EB, Hilgenfeld R, Weiss MS. Purification, characterization, and crystallization of alliinase from garlic. Arch Biochem Biophys 2002;402:192–200. [PubMed: 12051663]

Kurepin LV, Emery RJ, Pharis RP, Reid DM. Uncoupling light quality from light irradiance effects in *Helianthus annuus* shoots: putative roles for plant hormones in leaf and internode growth. J Exp Bot 2007;58:2145–2157. [PubMed: 17490995]

Ljung K, Hull AK, Celenza J, Yamada M, Estelle M, Normanly J, Sandberg G. Sites and regulation of auxin biosynthesis in *Arabidopsis* roots. Plant Cell 2005;17:1090–1104. [PubMed: 15772288]

Luccioni LG, Oliverio KA, Yanovsky MJ, Boccalandro HE, Casal JJ. Brassinosteroid mutants uncover fine tuning of phytochrome signaling. Plant Physiol 2002;128:173–181. [PubMed: 11788763]

Lukowitz W, Gillmor CS, Scheible WR. Positional cloning in *Arabidopsis*. Why it feels good to have a genome initiative working for you. Plant Physiol 2000;123:795–805. [PubMed: 10889228]

Mallory AC, Bartel DP, Bartel B. MicroRNA-directed regulation of Arabidopsis AUXIN RESPONSE FACTOR17 is essential for proper development and modulates expression of early auxin response genes. Plant Cell 2005;17:1360–1375. [PubMed: 15829600]

Matheron ME, Moore TC. Properties of an aminotransferase of pea (*Pisum sativum* L.). Plant Physiol 1973;52:63–67. [PubMed: 16658501]

Morelli G, Ruberti I. Shade avoidance responses. Driving auxin along lateral routes. Plant Physiol 2000;122:621–626. [PubMed: 10712524]

Morelli G, Ruberti I. Light and shade in the photocontrol of *Arabidopsis* growth. Trends Plant Sci 2002;7:399–404. [PubMed: 12234731]

Neff MM, Nguyen SM, Malancharuvil EJ, Fujioka S, Noguchi T, Seto H, Tsubuki M, Honda T, Takatsuto S, Yoshida S, Chory J. *BAS1*: A gene regulating brassinosteroid levels and light responsiveness in *Arabidopsis*. Proc Natl Acad Sci USA 1999;96:15316–15323. [PubMed: 10611382]

Peng J, Harberd NP. Gibberellin deficiency and response mutations suppress the stem elongation phenotype of phytochrome-deficient mutants of *Arabidopsis*. Plant Physiol 1997;113:1051–1058. [PubMed: 9112768]

Pierik R, Cuppens ML, Voesenek LA, Visser EJ. Interactions between ethylene and gibberellins in phytochrome-mediated shade avoidance responses in tobacco. Plant Physiol 2004;136:2928–2936. [PubMed: 15448197]

Reed JW, Nagpal P, Poole DS, Furuya M, Chory J. Mutations in the gene for the red/far-red light receptor phytochrome B alter cell elongation and physiological responses throughout *Arabidopsis* development. Plant Cell 1993;5:147–157. [PubMed: 8453299]

Sabatini S, Beis D, Wolkenfelt H, Murfett J, Guilfoyle T, Malamy J, Benfey P, Leyser O, Bechtold N, Weisbeek P, Scheres B. An auxin-dependent distal organizer of pattern and polarity in the *Arabidopsis* root. Cell 1999;99:463–472. [PubMed: 10589675]

Salter MG, Franklin KA, Whitelam GC. Gating of the rapid shade-avoidance response by the circadian clock in plants. Nature 2003;426:680–683. [PubMed: 14668869]

Sessa G, Carabelli M, Sassi M, Ciolfi A, Possenti M, Mittempergher F, Becker J, Morelli G, Ruberti I. A dynamic balance between gene activation and repression regulates the shade avoidance response in *Arabidopsis*. Genes Dev 2005;19:2811–2815. [PubMed: 16322556]

Snustad DP, Haas NA, Kopczak SD, Silflow CD. The small genome of *Arabidopsis* contains at least nine expressed beta-tubulin genes. Plant Cell 1992;4:549–556. [PubMed: 1498609]

Sorin C, Bussell JD, Camus I, Ljung K, Kowalczyk M, Geiss G, McKhann H, Garcion C, Vaucheret H, Sandberg G, Bellini C. Auxin and light control of adventitious rooting in *Arabidopsis* require ARGONAUTE1. Plant Cell 2005;17:1343–1359. [PubMed: 15829601]

Soto-Urzua L, Xochinua-Corona YG, Flores-Encarnacion M, Baca BE. Purification and properties of aromatic amino acid aminotransferases from *Azospirillum brasilense* UAP 14 strain. Can J Microbiol 1996;42:294–298. [PubMed: 8868238]

Steindler C, Matteucci A, Sessa G, Weimar T, Ohgishi M, Aoyama T, Morelli G, Ruberti I. Shade avoidance responses are mediated by the ATHB-2 HD-zip protein, a negative regulator of gene expression. Development 1999;126:4235–4245. [PubMed: 10477292]

Tam YY, Normanly J. Determination of indole-3-pyruvic acid levels in *Arabidopsis thaliana* by gas chromatography-selected ion monitoring-mass spectrometry. J Chromatogr A 1998;800:101–108. [PubMed: 9561757]

Tanaka S, Nakamura S, Mochizuki N, Nagatani A. Phytochrome in cotyledons regulates the expression of genes in the hypocotyl through auxin-dependent and -independent pathways. Plant Cell Physiol 2002;43:1171–1181. [PubMed: 12407197]

Truelsen TA. Indole-3-pyruvic acid as an intermediate in the conversion of tryptophan to indole-3-acetic acid. I. Some characteristics of tryptophan transaminase from mung bean seedlings. Physiologia Plantarum 1972;26:289–295.

Woodward AW, Bartel B. Auxin: regulation, action, and interaction. Ann Bot (Lond) 2005;95:707–735. [PubMed: 15749753]

Zhao Y, Christensen SK, Fankhauser C, Cashman JR, Cohen JD, Weigel D, Chory J. A role for flavin monooxygenase-like enzymes in auxin biosynthesis. Science 2001;291:306–309. [PubMed: 11209081]

Zhao Y, Hull AK, Gupta NR, Goss KA, Alonso J, Ecker JR, Normanly J, Chory J, Celenza JL. Trp-dependent auxin biosynthesis in *Arabidopsis*: involvement of cytochrome P450s CYP79B2 and CYP79B3. Genes Dev 2002;16:3100–3112. [PubMed: 12464638]

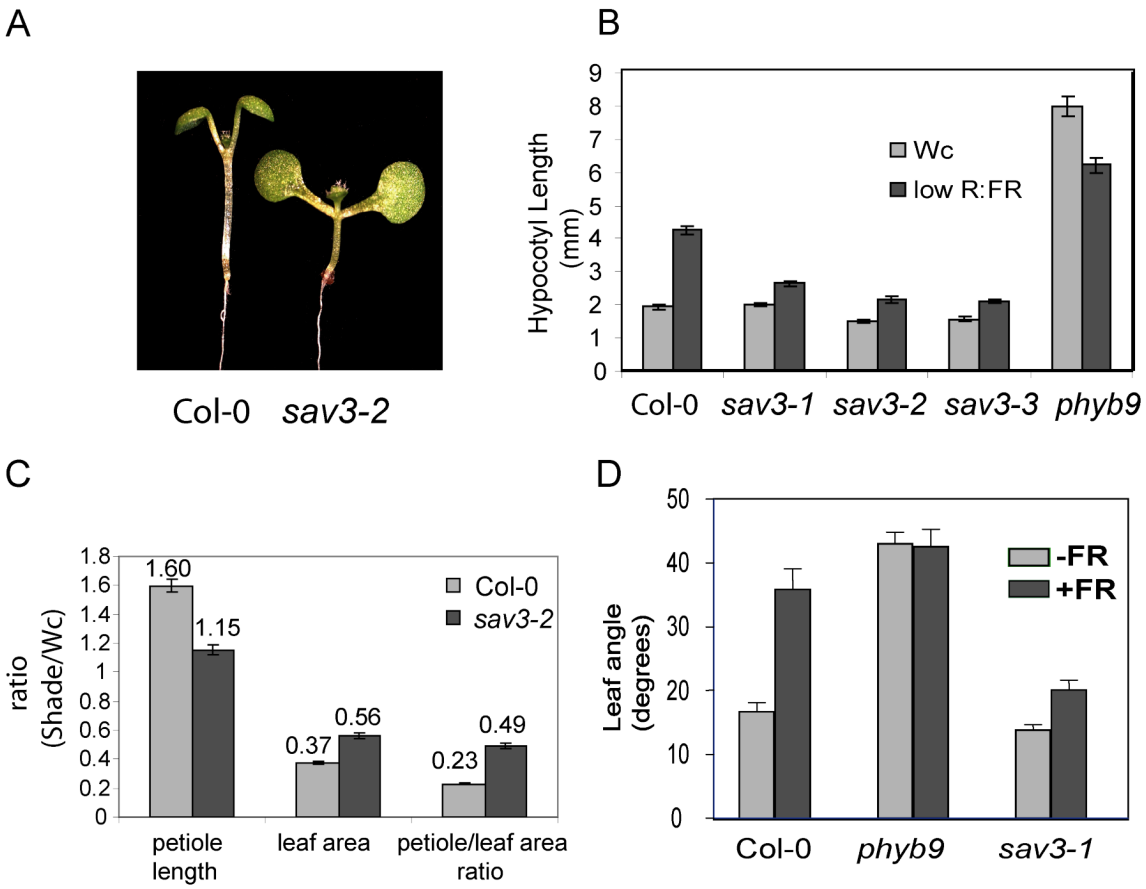

Figure 1. Phenotypic Characterization of *sav3* Mutants

(A) Hypocotyl phenotype of *sav3* mutants. 5-day old seedlings were treated with Wc or simulated shade for 3 days. Representative seedlings of shade-treated WT Col-0 and *sav3-2* are shown on the left; hypocotyl length is quantified on the right. *phyB9* is a null allele of *PHYB*.

(B) Leaf area and petiole length phenotypes of *sav3-2*. 7-day-old seedlings were treated with Wc or simulated shade for two weeks. Petiole length and leaf area of the first set of true leaves were measured.

(C) Leaf hyponasty phenotype of *sav3-1*. Four-week-old plants were cultivated in a greenhouse and then exposed for 10 days to supplemental FR irradiation (see supplement for details).Error bars represent standard error of the mean (SEM).

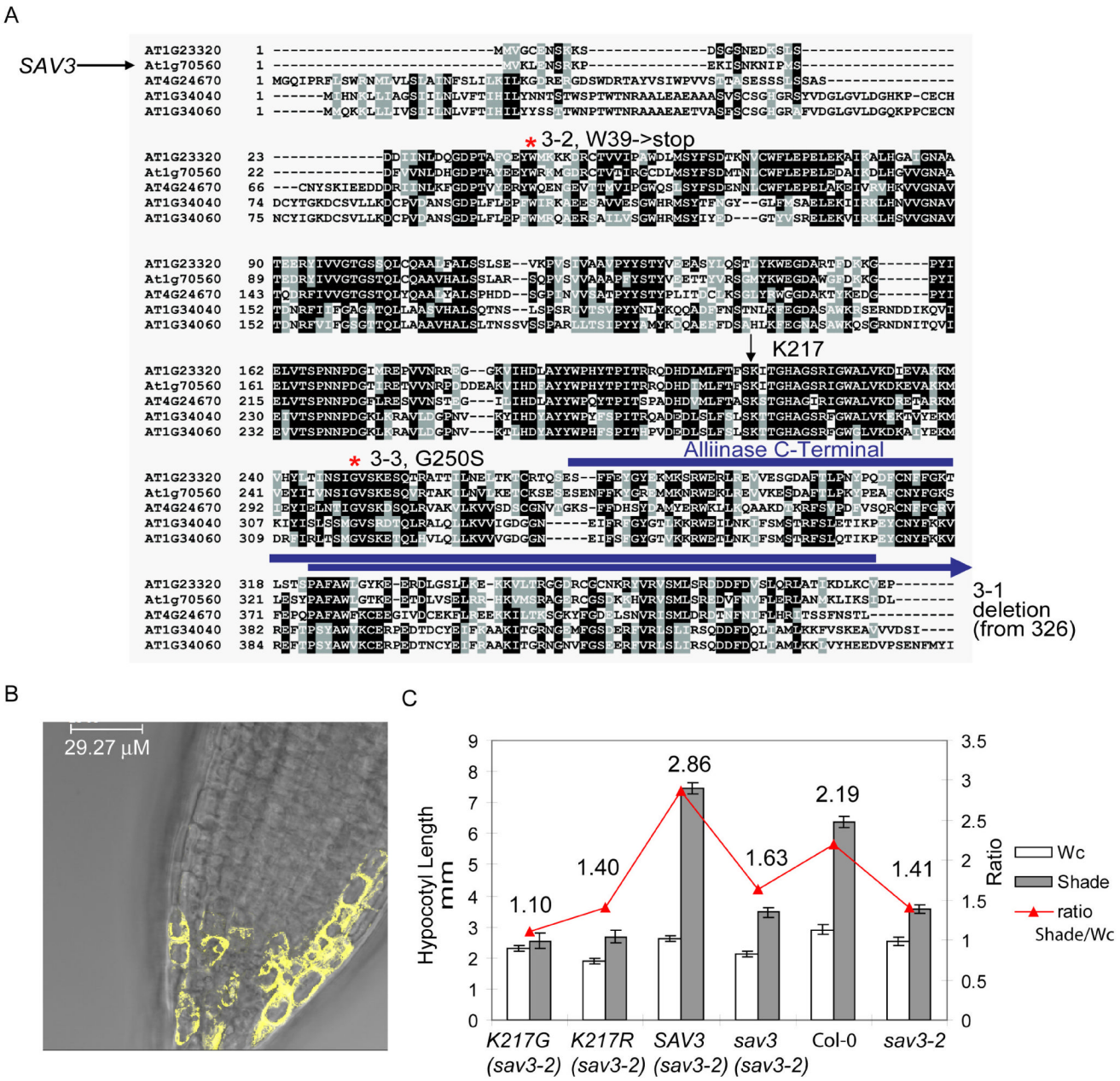

Figure 2. *SAV3* Encodes an Enzyme with an Alliinase C-Terminal/Aminotransferase Domain

(A) Protein alignment of *Arabidopsis* SAV3 family. The alliinase C-terminal domain is marked by a blue line. K217 is the PLP binding site.

(B) Cytoplasmic localization of SAV3-YFP in root meristem cells. SAV3-YFP was expressed stably in *sav3-1* under the control of the CaMV 35S promoter. The YFP fusion protein was visualized using a Leica confocal microscope.

(C) Complementation test using *SAV3* genomic DNA fragment (*SAV3*) or mutant forms of *SAV3* (*K217G*, *K217R* or an N-terminal truncation containing the first 130 a.a.). At least 3 independent transgenic lines were used for characterization of SAV3 localization and phenotypes. Mean values of more than 12 seedlings are shown; error bars represent SEM.

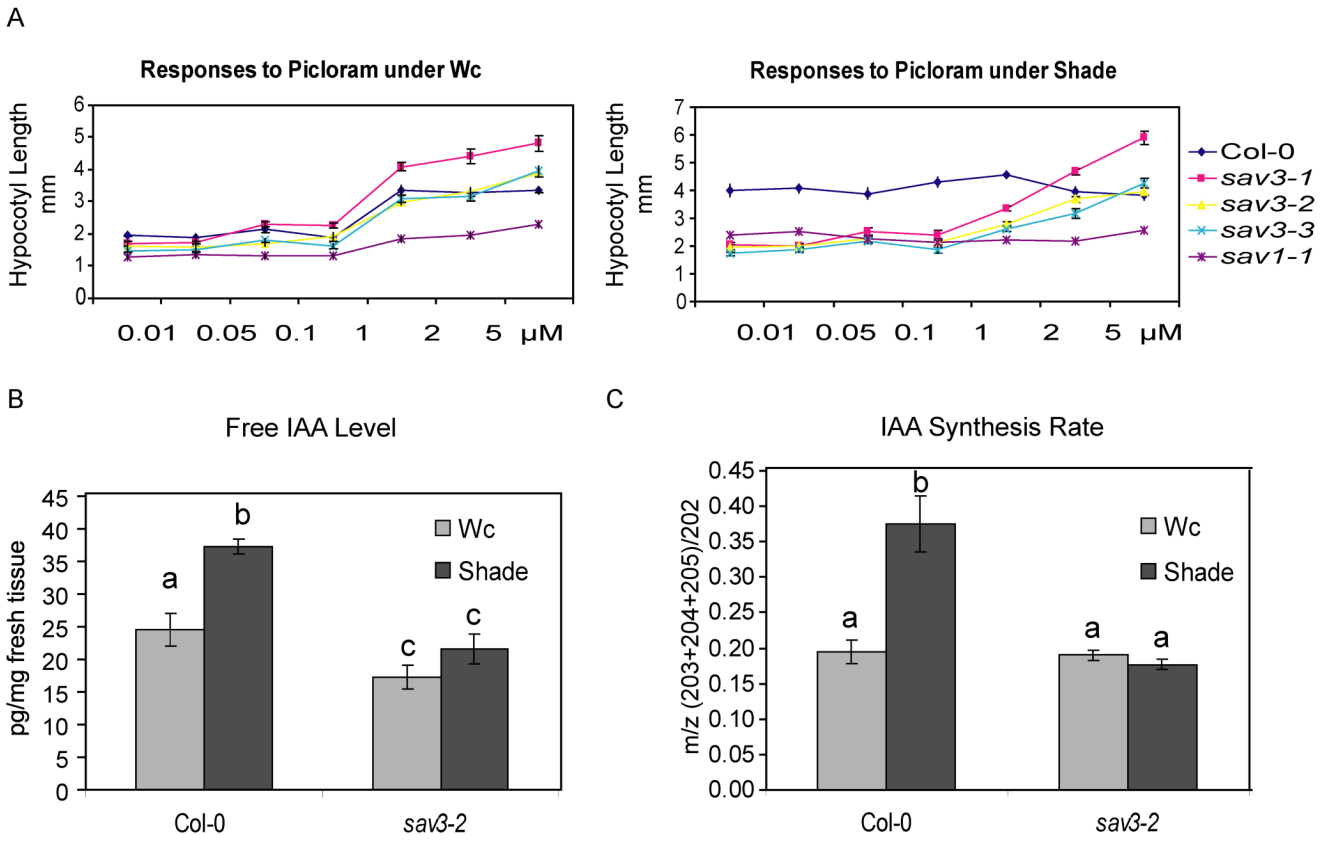

Figure 3. *Sav3* Mutants are Defective in Auxin Biosynthesis

(A) Responses of *sav3* to the auxin analog, picloram. Seedlings were grown in Wc on plates with picloram for 3 days and then moved to Wc or simulated shade for 3 days. Error bars represent SEM.

(B) *sav3* seedlings have reduced IAA levels in Wc and shade light. WT and *sav3* were grown in Wc and moved to Wc or shade for 1 hour.

(C) *sav3* has lower rates of IAA biosynthesis in the shade. Seedlings were grown for 5 days in Wc and then incubated in ½ MS with 30% $^{2}H_{2}O$ and treated with Wc or shade for 2 hours. Samples with the same letter are not significantly different based on one-way ANOVA followed by a two-sided t-test at $P<0.01$.

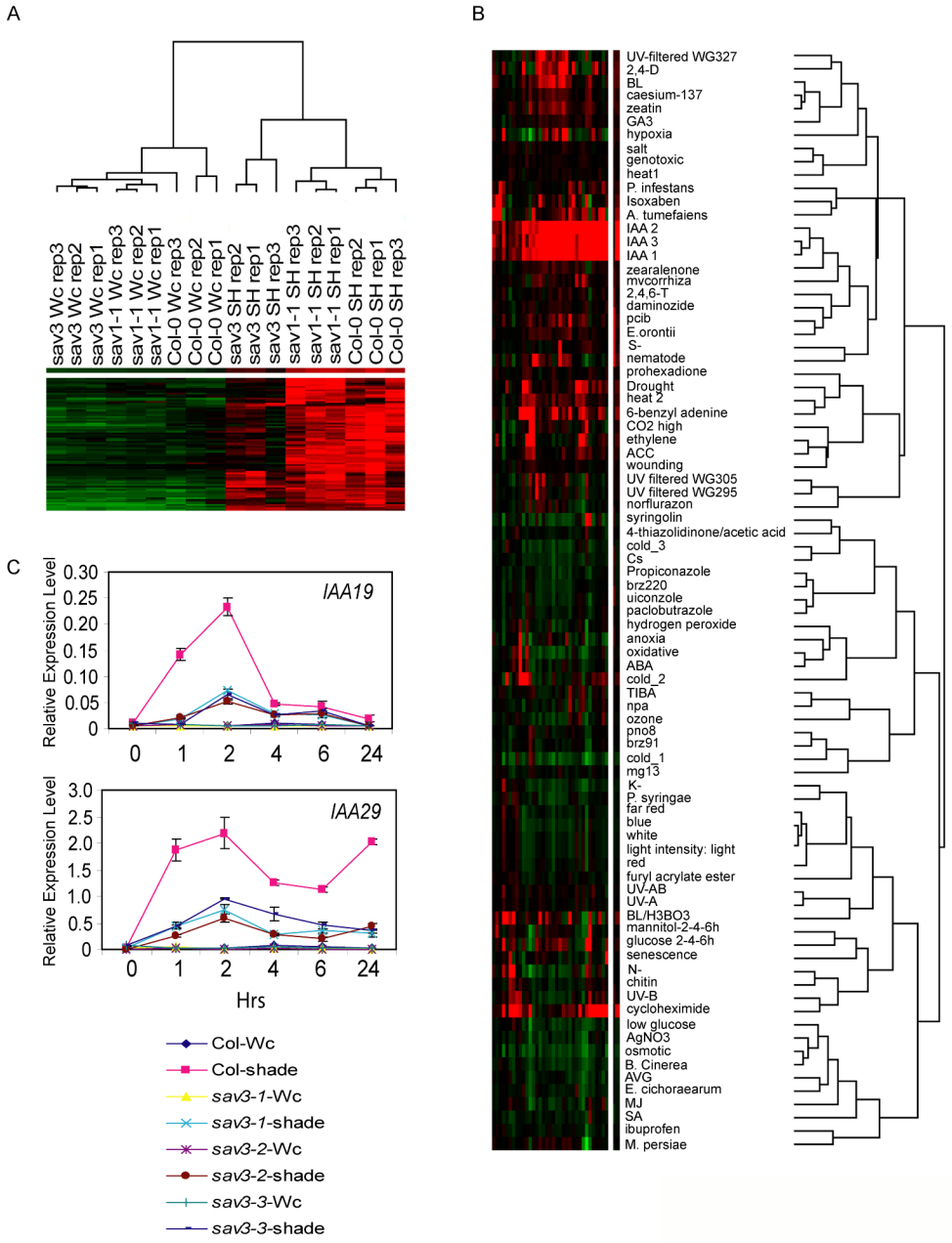

Figure 4. Global Expression Analysis of *sav3* Implicates a Role for SAV3 in Auxin Response

(A) Expression pattern of shade-induced genes.

(B) Co-response analysis of SAV3-dependent, shade up-regulated genes. Expression data of each gene was normalized and medium centered using Cluster, and visualized by Treeview (http://rana.lbl.gov/EisenSoftware.htm). Green and red represent lower and higher expression level as compared to the median value, respectively.

(C) Quantification of *IAA19* and *IAA29* expression using quantitative RT-PCR. Relative expression level as compared to a reference gene (At2G39960) is shown. Data are presented as mean values from 3 replicates +/− SEM.

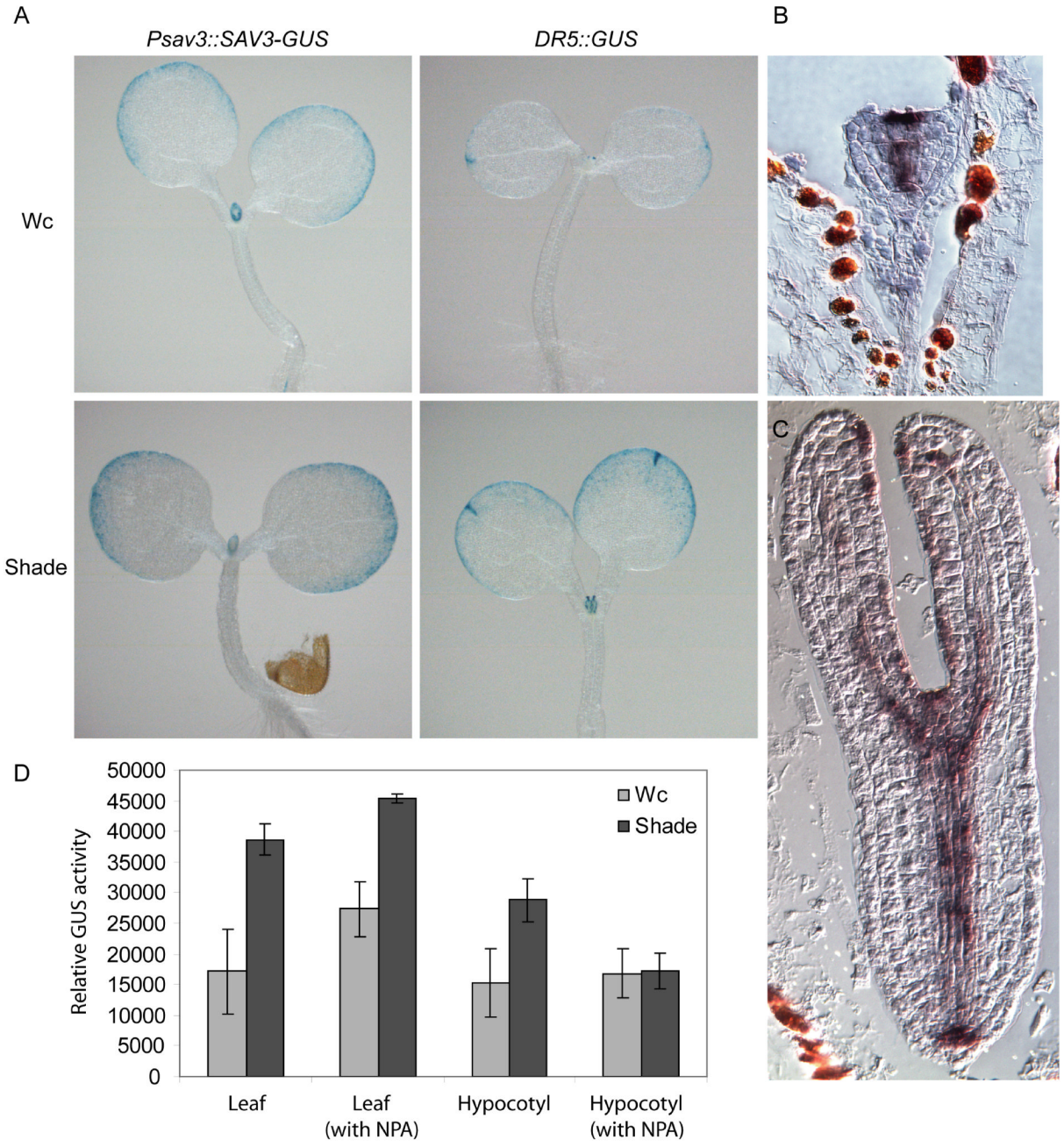

Figure 5. *SAV3* Expression is Dynamic

(A) *SAV3* is expressed predominantly in the leaf margins. Expression patterns of P_{SAV3}n::*SAV3-GUS* and DR5::*GUS* are shown. 5-day-old seedlings were treated with Wc or shade for 8 hours. (B) and (C) *in situ* hybridization results show *SAV3* is expressed during the heart (B) and torpedo (C) stages of embryogenesis.

D) Shade-induced increase in *DR5-GUS* expression is dependent on *SAV3* expression in leaves and functional auxin transport. 5-day old seedlings were pre-treated with 5 μM of NPA by submerging roots in NPA solution for 30 min and then subjected to Wc or shade for 4 hrs. Relative GUS activity was calculated by normalizing to the chlorophyll content. Mean values from 3 replicates are shown; error bars represent SEM. T-test assuming equal variance was

carried out for Wc and shade-treated sample pairs. Comparing Wc and shade treated samples, only NPA treated hypocotyls shows no significant difference (using $P<0.05$ as cut-off).

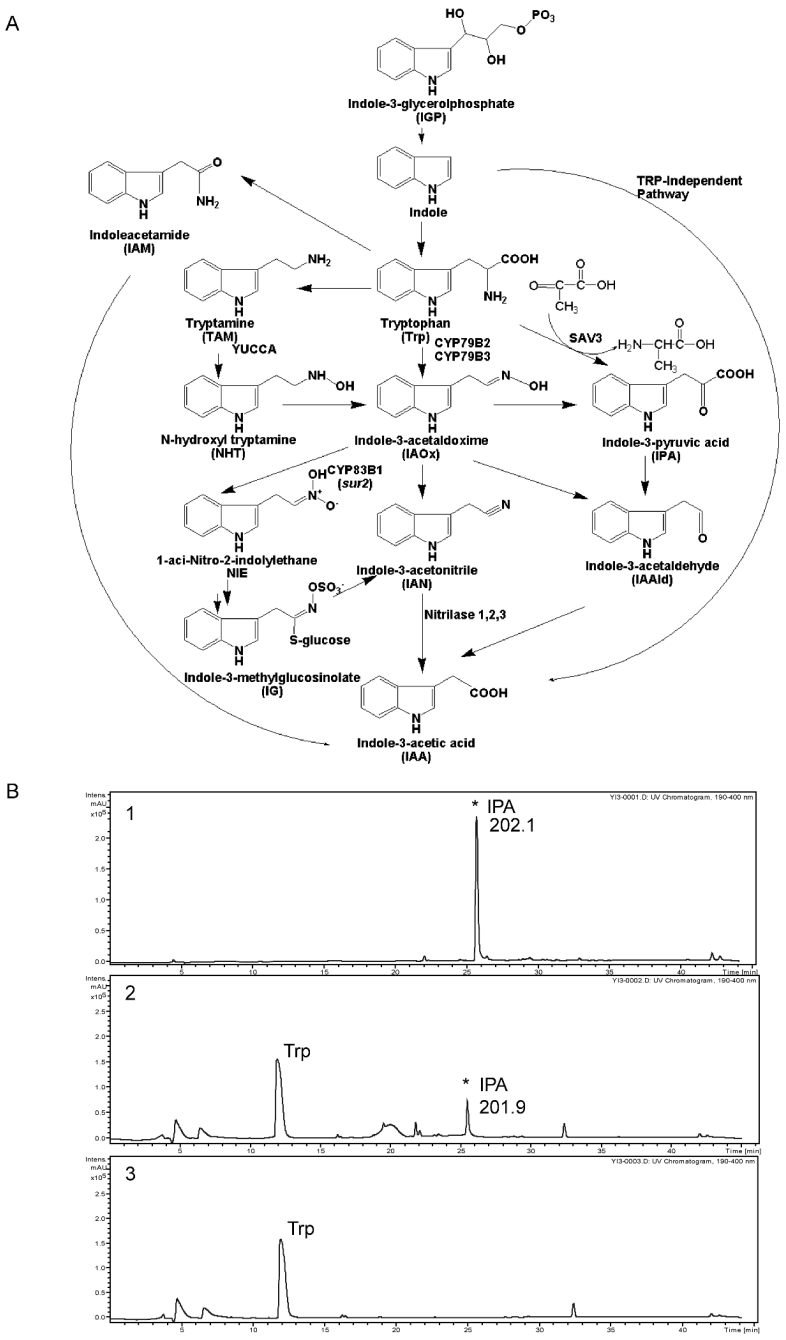

Figure 6. SAV3 is a Trp Aminotransferase Involved in Auxin Biosynthesis

(A) Schematic diagram of the proposed IAA biosynthetic pathways.

(B) Identification by LC/MS of indole pyruvic acid (IPA) as the product of SAV3 when L-Trp is used as substrate. Shown are the UV-chromatogram profiles of IPA control (1), reaction mixture (2) and reaction mixture without SAV3 (3). The number shown is the calculated mass of IPA.

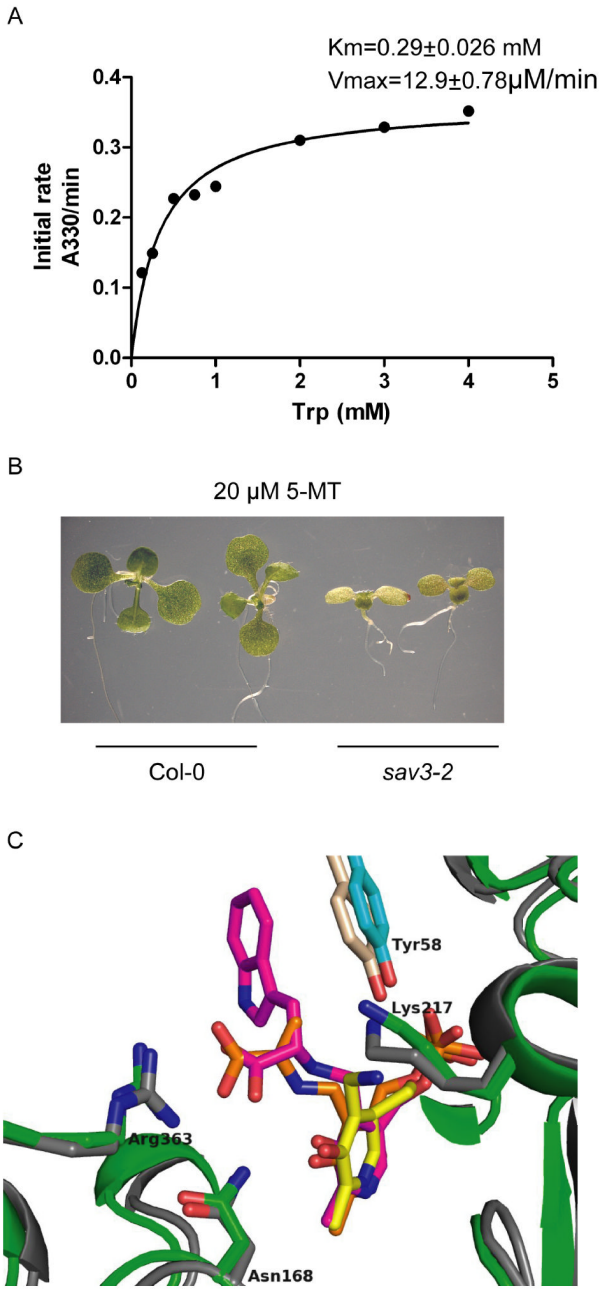

Figure 7. Enzymatic Characterization of SAV3

(A) Determination of Km and Vmax of SAV3 to L-Trp.

(B) *sav3-2* is hypersensitive to 5-MT. Seedlings were grown on ½ MS medium supplemented with 20 μM 5-MT for 9 days in Wc.

(C) Superimposed structure of SAV3 and alliinase active sites. SAV3 monomers are represented as green and cyan ribbons. Alliinase monomers are represented in grey and wheat ribbons (PDB code: 2hox). Labels are those of SAV3 residues. Pyridoxamine phosphate (PMP) as observed in SAV3 structure is represented by yellow sticks. aminoacrylate-PLP as observed in alliinase structure is represented by orange sticks. Trp-PLP from an *in silico* docking experiment is represented as magenta sticks.